Hindawi Publishing Corporation
Journal of Cancer Research
Volume 2015, Article ID 762716, 15 pages
http://dx.doi.org/10.1155/2015/762716

Research Article

Molecular Docking Study Characterization of Rare Flavonoids at the Nac-Binding Site of the First Bromodomain of BRD4 (BRD4 BD1)

Karthik Dhananjayan

Department of Pharmacology, Amrita School of Pharmacy, Amrita Vishwa Vidyapeetham University, AIMS Health Sciences Campus, Kochi, Kerala 682041, India

Correspondence should be addressed to Karthik Dhananjayan; karthikdcology@gmail.com

Received 27 September 2014; Revised 13 February 2015; Accepted 13 February 2015

Academic Editor: Daizo Yoshida

ε-N-Acetylation of lysine residues (Kac) is one of the most frequently occurring posttranslational modifications (PTMs) which control gene transcription and a vast array of diverse cellular functions. Bromodomains are epigenetic regulators involved in posttranslational modification. *In silico* docking studies were carried out to evaluate the binding potential of selected rare flavonoids on to Nac binding site of BD1 domain of BRD4 BET family proteins. Rare flavonoids like 3-O-acetylpinobanksin, naringenin triacetate, and kaempferol tetraacetate were found to occupy the WPF shelf and at the same time they exhibited a better binding affinity with multiple crystal structures of first bromodomain BRD4 (BRD4 BD1) when compared with the known inhibitors.

1. Introduction

The recent discovery of promising small molecule inhibitors for a class of nonenzymatic chromatin regulators, the BET bromodomains, suggests that future drug discovery for epigenetic therapy will involve the modulation of protein-protein interactions and multiprotein complexes. Also, it is expected that target-based discovery strategies will be increasingly complemented by approaches based on chemical probes generated by phenotypic or mechanistic cell based screening [1].

The bromodomain (BD) and extra terminal (BET) proteins, which comprise four members in human viz., BRD2, BRD3, BRD4, and the testis-specific BRDT [2] with each containing two N-terminal Bromodomains (BD). BRD4 and BRD2 are key mediators of transcriptional elongation by recruiting the positive transcription elongation factor complex (P-TEFb). The P-TEFb core complex is composed of cyclin-dependent kinase-9 (CDK9) and its activator cyclin T. CDK9 phosphorylates the RNA polymerase II (RNAPII) C-terminal domain, a region that contains 52 heptad repeats. RNAPII undergoes sequential phosphorylation at Ser5 during promoter clearance and at Ser2 by P-TEFb at the start of elongation. It has been shown that BRD4 couples P-TEFb to acetylated chromatin through its BRDs. Interestingly, in contrast to other BRD containing proteins and transcription factors, BET proteins remain associated with condensed and hypoacetylated mitotic chromosomes [3] suggesting a role in epigenetic memory [4, 5].

Acetylation of lysine residues is a posttranslational modification with broad relevance to cellular signaling and disease biology. The principal readers of ε-N-acetyl-lysine (Kac) marks are bromodomains (BRDs), which are a diverse family of evolutionary conserved protein-interaction modules. The conserved BRD fold contains a deep, largely hydrophobic acetyl-lysine binding site, which represents an attractive pocket for the development of small pharmaceutically active molecules [6].

The bromodomain-containing protein-4 (BRD4) is a class of transcriptional regulators whose members are present in animals, plants, and fungi [7]. The BET proteins typically have two tandem N-terminal bromodomains followed by an ET domain. As predicted by the presence of bromodomains, these proteins have been found to be associated with acetylated chromatin. BET proteins are involved in diverse cellular phenomena such as meiosis, cell-cycle control, and homeosis and have been suggested to modulate chromatin structure

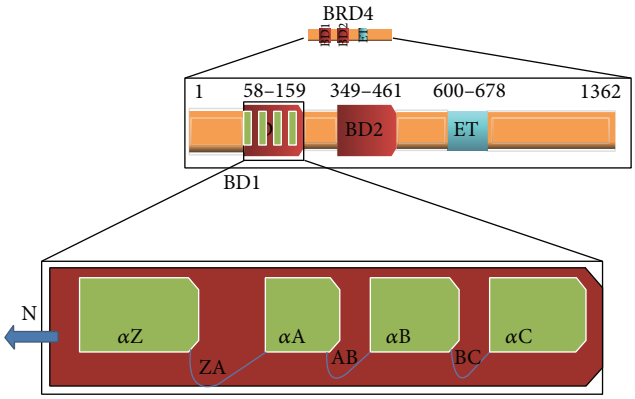

Figure 1: Schematic diagram of human BRD4 with two N-terminal bromodomains (BD1 and BD2) with an extra terminal (ET) domain. The emphasized bromodomain-1 (BD1) shows N-terminus, alpha-Z, ZA loop, alpha-A, AB loop, alpha-B, BC loop, and alpha C. The schematic diagram is based on as per the information from [49].

and affect transcription via a sequence-independent mechanism [8]. Figure 1 shows the schematic diagram of BRD4 with BD1, BD2 domains, and an extra terminal domain (ET).

Every first bromodomain BRD4 (BRD4 BD1) of BET has an N-terminus, alpha-Z helix, alpha-A helix, ZA loop, AB loop, alpha-B helix, BC loop, and alpha C helix. In these, the four identified distinct BET bromodomains have 80% similar amino acid sequences in BD1 domain and at the same time they conserve some amino acid residues.

ε-N-Acetylation of lysine residues (Kac) is one of the most frequently occurring posttranslational modifications (PTMs) in proteins [9]. The secondary structure with helices and loops is shown in Figure 2 along with hydrophobic site for histone deacetylation (Kac site) which is projected.

Bromodomain inhibitors introduced so far are mostly BRD4 BD1 inhibitors. Among them, JQ1 is a BRD4 bromodomain inhibitor and it is highly active against human leukemia OCI-AML3 mutation lines such as nucleophosmin (NPM1) and DNA methyltransferase 3 (DNMT3A). JQ1 causes caspase 3/7-mediated apoptosis and DNA damage response in these cells. JQ1 prevented BRD4-mediated recruitment of p53 to chromatin targets following its activation in OCI-AML3 cells resulting in cell cycle arrest and apoptosis in a c-MYC-independent manner [10]. GSK525762 binds to the acetylated lysine recognition motifs on the bromodomain of BET proteins, thereby preventing the interaction between the BET proteins and acetylated histone peptides. This disrupts chromatin remodeling and gene expression. Prevention of the expression of certain growth-promoting genes may lead to an inhibition of tumor cell growth. GW841819X displayed activity in vivo against NUTmidline carcinoma, multiple myeloma, mixed-lineage leukemia, and acute myeloid leukemia [11]. Benzodiazepines and I-BET762 are BET bromodomain inhibitors now in clinical trial for nuclear protein in testis (NUT) midline carcinoma and other cancers [12–14]. MS435 and MS436 effectively inhibit BRD4 activity in NF-κB-directed production of nitric oxide and proinflammatory cytokine interleukin-6 in murine macrophages. MS435 and MS436 represent a new class of bromodomain inhibitors where MS436 is the best inhibitor [15].

X-ray crystallography shows that the chromen-4-one scaffold represents a new bromodomain pharmacophore and establishes LY294002 as a dual kinase and BET bromodomain inhibitor, whereas LY303511 exhibits anti-inflammatory and antiproliferative effects similar to the recently discovered BET inhibitors. LY294002 is a 2-morpholin-4-yl-7-phe-nyl-4H-chromen-4-one. Proteins BRD2, BRD3, and BRD4 comprise a family of targets structurally unrelated to PI3K [16]. Figure 3 shows the structures of some known inhibitors of the first bromodomain of BRD4 (BRD4 BD1).

On this basis, some acetyl forms of flavonoids were selected and their binding affinity was analyzed. Selection of rare flavonoids is based on the structural aspects. Figure 4 shows the selective ligands under investigation. To support Lipinski's rule of five, Table 1 was listed out with chemical properties of ligands (selective rare flavonoids) like molecular formula, molar mass, Log P, and so forth. This study was aimed at understanding the differences in the presence of acetyl groups at various positions around the 1, 4-benzopyrone nucleus. In such perspective, acetyl form of naringenin, jaceidin, pinobanksin, kaempferol, artemetin, and hydroxy flavone were identified and carried over for *in silico* screening against bromodomains. The ligands were examined for Lipinski's rule of five. Rule of five is used to determine if a chemical compound, with a certain pharmacological or biological activity, has some properties that would make it a likely orally active drug in humans. It explains a molecule's pharmacokinetic properties, namely, absorption, distribution, metabolism, and excretion, but this rule lacks to explain whether the molecule would be pharmacologically active. In the discovery setting "the rule of 5" predicts that poor absorption or permeation is more likely when there are more than 5 hydrogen bond donors, 10 hydrogen bond acceptors, the molecular weight is greater than 500, and the calculated Log P (CLogP) is greater than 5 [17]. According to the drug likeness properties, the ligands showed zero violation of the Lipinski rule of five, except kaempferol tetraacetate and jacedin triacetate.

In this study, the specific bromodomains BD1 domain of BRD4 BET family was selected. For validation, the specific pdb crystal structure with its cocrystallized ligand was redocked. Then a set of crystal structures with their cocrystallized ligands (known inhibitors) were evaluated for their effectiveness in binding. Multiple crystal structures of first bromodomain (BD1) of BRD4 BET family with different resolutions was downloaded from RCSB protein data bank and investigating ligands (rare flavonoids) with lowest binding energy was re-evaluated on different crystal structures.

2. Materials and Methods

The crystal structures of bromodomains used for evaluation in this study were obtained from RCSB protein data bank [18]. Ligands were designed using Chemsketch [19, 20] and

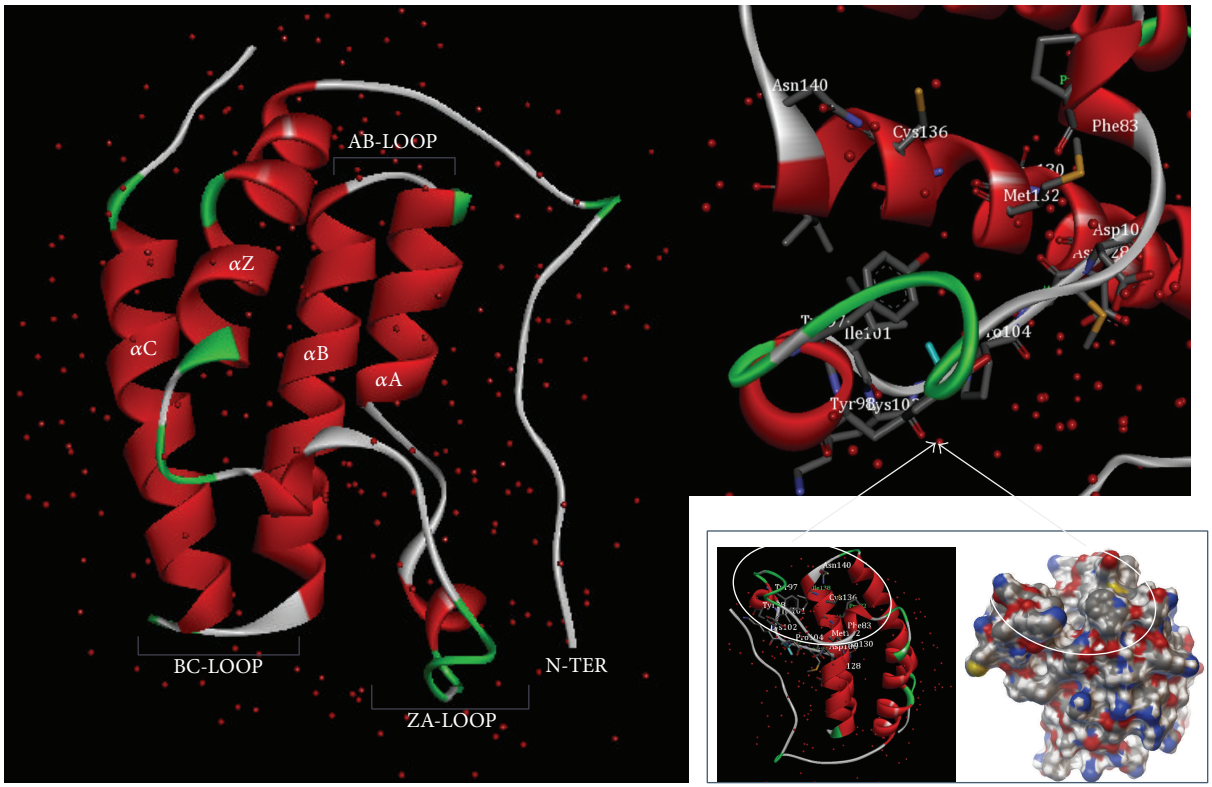

Figure 2: Secondary structure of bromodomain BD1-BRD4 with water molecules showing N-terminus, α-Z helix, α-A helix, ZA loop, AB loop, α-B helix, BC loop, and α-C helix. Adjacent image with white arrows below shows a secondary structure and surface diagram which in turn emphasizes a circled area of hydrophobic sites. Diagram of secondary structure generated using Accelrys' discovery studio 4.0 [25].

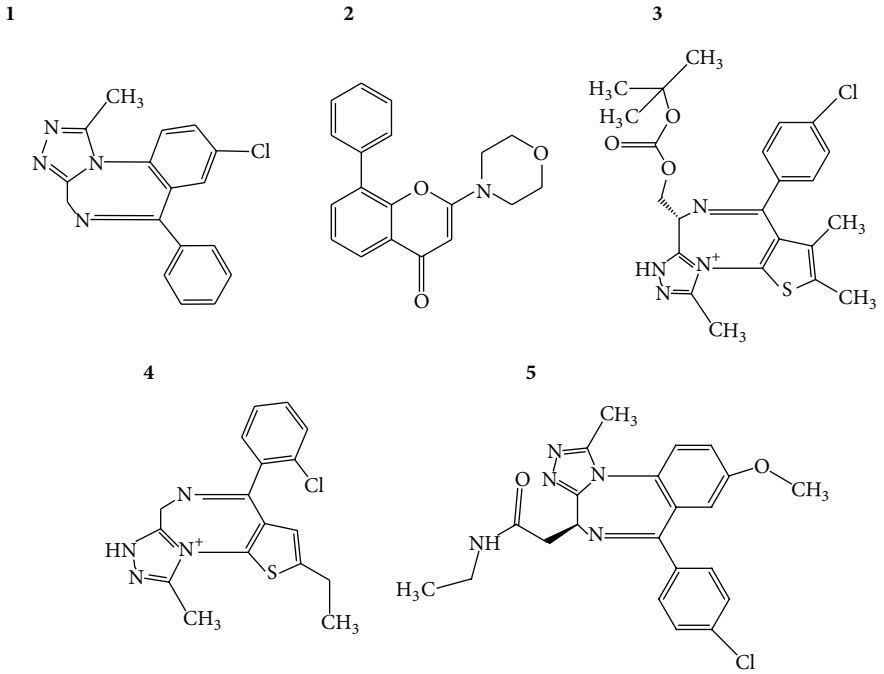

Figure 3: Known inhibitors. (**1**) Midazolam, (**2**) LY294002, (**3**) JQ1, (**4**) I-BET 762, and (**5**) GSK525762 (IBET).

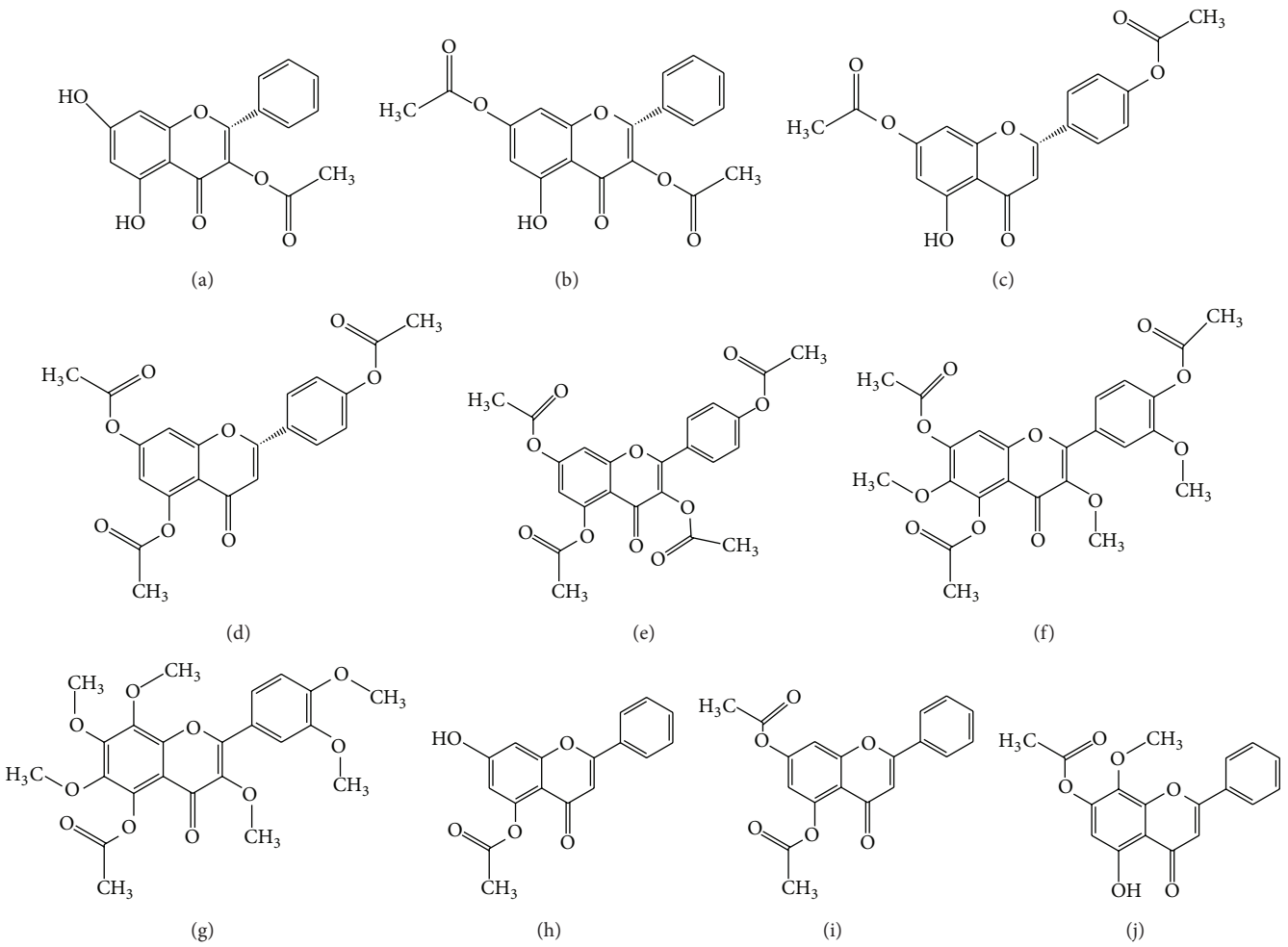

Figure 4: Rare flavonoids (a) 3-O-acetylpinobanksin, (b) 3,7-O-acetylpinobanksin, (c) naringenin diacetate, (d) naringenin triacetate, (e) kaempferol tetraacetate, (f) jaceidin triacetate, (g) artemetin acetate, (h) 5-acetoxy-7-hydroxyflavone, (i) 5,7-diacetoxyflavone, and (j) 5-hydroxy-7-acetoxy-8-methoxy flavone.

Table 1: Table showing the list of ligands (with CAS number) used for investigation and their chemical properties.

Serial number	Ligand	CAS number	Molecular formula	Molecular weight	Log *P*	H-bond donors	H-bond acceptors	Rule of 5 number of violations	Torsions
01	3-O-Acetylpinobanksin	52117-69-8	$C_{17}H_{14}O_6$	314.28	3.85 ± 0.41	2	6	0	5
02	Naringenin triacetate	3682-04-0	$C_{21}H_{18}O_8$	398.36	2.14 ± 0.80	0	8	0	7
03	Kaempferol tetraacetate	16274-11-6	$C_{23}H_{18}O_{10}$	454.38	1.16 ± 1.36	0	10	1	9
04	Artemetin acetate	95135-98-1	$C_{22}H_{22}O_9$	430.40	1.84 ± 1.45	0	9	0	8
05	Naringenin-4′,7-diacetate	18196-13-9	$C_{19}H_{16}O_7$	356.32	3.51	1	7	0	6
06	3,7-O-Acetylpinobanksin	103553-98-6	$C_{19}H_{16}O_7$	356.08	4.10 ± 0.44	1	7	0	6
07	Jaceidin triacetate	14397-69-4	$C_{24}H_{22}O_{11}$	486.24	0.647	0	11	1	10
08	5-Hydroxy-7-acetoxy-8-methoxy flavone	95480-80-1	$C_{17}H_{14}O_6$	326.30	2.942	1	6	0	5
09	5,7-Diacetoxy flavone	6665-78-7	$C_{19}H_{14}O_6$	338.31	4.10 ± 0.44	0	6	0	5
10	5-Acetoxy-7-hyroxy flavone	132351-58-7	$C_{17}H_{12}O_5$	296.27	3.07 ± 0.87	1	5	0	4

The chemical properties mentioned above for the ligands are available from the link: http://www.rsc.org.

designed ligands were optimized for their geometry with MOPAC [21] in Chem3D Ultra 9.0 platform [22], molecular docking was performed using LeDock [23], and overlapping analysis was done with PyMOL [24]. Nonbond interactions of ligands with bromodomains were viewed through Accelrys' discovery studio 4.0 [25] and ligand map was generated using Molegro Molecular viewer 2.5 [26, 27], Ligplot is generated using Ligplot plus 1.4.5 [28].

2.1. Ligand Preparation Using MOPAC. MOPAC (Molecular Orbital Package) is a semiempirical quantum chemistry program based on Dewar and Thiel's NDDO approximation. MOPAC uses semiempirical theory to calculate the electronic part, in order to obtain molecular orbitals, the heat of formation, and its derivative with respect to molecular geometry [21]. MOPAC in Chem3D Ultra 9.0 employs AM1 (Austin Model 1) method and closed shell wave function to minimize energy to minimum RMS gradient of 0.100. AM1, belong to the family of NDDO (Neglect of Diatomic Differential Overlap) methods. In these methods, all terms arising from the overlap of two atomic orbitals which are on different centers or atoms are set to zero. As this is not the forum for developing the ideas of Hartree-Fock theory [29], knowledge about the derivation of the Roothaan-Hall equations [30] will be assumed and description of the methods will start with the final equations. Properties like heat of formation, gradient norm, charges, cosmos ovation in water, electrostatic potential, molecular surfaces, spin density, hyperfine coupling constants, and polarizabilities were solved and, additionally, Mulliken charges were calculated. Mulliken charges [31] provide means of estimating partial atomic charges and are routinely used as variables in linear multiple regression QSAR procedures. 3D structures obtained after MOPAC calculations were visualized through Accelrys' discovery Studio 4.0.

2.2. Docking Software. LeDock (http://www.lephar.com/) is developed for fast, flexible, and accurate docking of small molecule ligands into a protein target with extremely simplified interface. LeDock utilizes a combination of simulated annealing and genetic algorithm for the optimization of position, orientation, and rotatable bonds of the ligand [23]. Its built-in scoring function, adapted from a transferable and accurate energy function [32], mainly consists of Vdw interaction energy and a unique empirical-based hydrogen bonding energy.

2.3. First Bromodomain of BRD4 (BRD4 BD1) Crystal Structure Energy Optimization. Different crystal structures of first bromodomain of BRD4 (BRD4 BD1) of BET family proteins were optimized for their geometry with Open Babel 2.3.2 [33, 34]. It uses a general Amber force field (GAFF) for energy minimization. GAFF is designed to be compatible with existing Amber force fields for proteins and nucleic acids and has parameters for most organic and pharmaceutical molecules that are composed of H, C, N, O, S, P, and halogens. It uses a simple functional form and a limited number of atom types but incorporates both empirical and heuristic models to estimate force constants and partial atomic charges [35]. Optimized crystal structures were utilized for docking evaluation.

2.4. Validation of Computational Molecular Docking. To know the accuracy of molecular docking, the cocrystallized ligand has to be retrieved and redocked onto the active site. Root-mean-square deviation (RMSD) between the docked structure and the original conformation of the inhibitor in each complex was calculated. Crystal structure (4CFK) with its cocrystallized ligand was selected and validation was performed.

2.5. Docking Methodology

2.5.1. Preparation of Protein Molecule Using Lepro. Lepro is an advanced program in refining the protein molecule. It has a dual advantage in detecting the binding site and as well as removal of water molecules. Even though the binding site (the space search (grid) for the ligand) is recognized in the presence of a cocrystallized ligand, it conserves precision. The protein molecule is loaded and hydrogen is added prior to docking. Lepro writes refined protein molecule as a ".pdb" file (e.g., pro.pdb), but docking parameters as ".in" file (dock.in). Pro.pdb and dock.in are the files needed in order for LeDock to carry out its docking evaluation. After adding hydrogen, the binding site was determined.

2.6. Docking of the Ligands Using LeDock. Refined protein molecule (pro.pdb) and docking input files (dock.in) were uploaded before selecting a ligand. The ligand in a SYBYL MOL2 (ligand.mol2) format is an only ideal file that can be recognized by the LeDock. After constructing all necessary files, the docking is started using start "docking icon." The number of poses generated and their binding affinity (docking score) will be generated. Maximum of 20 poses will be generated depending upon torsions in the ligands.

3. Results and Discussion

As quoted above, LeDock is a built-in scoring function adapted from a transferable and accurate energy function mainly consisting of Vdw interaction energy and a unique empirical-based hydrogen bonding energy. The docking score is calculated as given in (1). Consider

$$\Delta G = \alpha \Delta E_{ff} + \beta P_{\mathrm{HB}} + \gamma, \tag{1}$$

where ΔG is binding energy; ΔE_{ff} is interaction energy; P_{HB} is hydrogen bonding penalty; α, β, and γ are fitting parameters.

LeDock generates 20 different poses of each ligand depending upon torsions. There were no less than 6 poses on the above said criteria at the vicinity of the binding site for the investigated ligands

3.1. Validation of Molecular Docking. Validation of docking methodology was performed in order to measure the reliability of molecular docking. Root-mean-square deviation

Table 2: Validation set showing the docking score of known inhibitors onto the crystal structure of multiple BRD4 (BD1).

Serial number	Known inhibitors	PDB code	Resolution of BRD Å	Number of water molecules	RMSD (Å)	Docking score kcal/mol	Amino acids interacted through hydrogen bonding	H-bond length Å
1	MIDAZOLAM	3U5J	1.60	349	0.92	−5.08	Asn140 Asn140 Cys136	3.91 2.83 3.84
2	LY294002	4CFK	1.55	238	0.85	−5.73	Asn40	2.71
3	JQ1	3MXF	1.60	341	0.94	−6.52	Cys136 Asn140	4.08 3.23
4	I-BET762	4C66	1.87	119	0.97	−6.00	Asn140 Asn140 Cys136 Tyr97	4.21 3.10 4.10 4.22

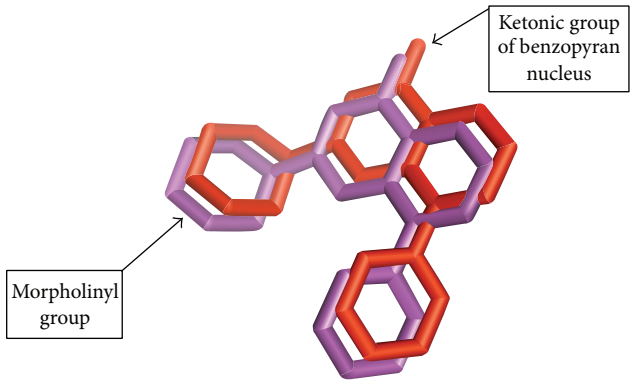

Figure 5: Validation of molecular docking (LeDock). The magenta shows the native ligand (LY294002) pose retrieved from the crystal structure 4CFK and red colour shows the docked pose of the ligand (LY294002) using LeDock. (the docked files have been displayed using PyMOL and the retrieved ligand from cocrystallized structure in its conformation has been loaded to superimpose on each other).

(RMSD) between the docked structure and the original conformation of the inhibitor in each complex was calculated. If the RMSD of the docked pose is less than or equal to 1.0 Å from the experimentally observed conformation, the prediction is regarded to be successful.

LY294002 is a chromen-4-one compound exhibiting a docking score of −5.30 kcal/mol. Among the selective ligands, a prediction has been made to show their binding affinity towards gorge area. Figure 5 shows the docked conformation and original conformation of LY294002 with their respective docked energy.

In LY294002, the major functional group involved in hydrogen bond interaction was oxygen atom of ketonic (–C=O) group at C5 position and the rest of the aromatic rings interaction dealt with hydrophobic interaction. There was only a slight variation in occupying the WPF shelf, which can be evidenced from the ring shift and torsional shift of the redocked ligand from native ligand retrieved from the crystal structure. This reliability holds strong to perform the docking analysis with investigational ligands.

Asn140 donates its hydrogen to make a bond with oxygen atom of LY294002 at C5 position containing ketonic group. The former interaction of redocked ligand caused a shift of 0.15 Å when compared with the cocrystallized ligand. Table 2 shows the distance of H-bond formed by the cocrystallized ligand and the redocked ligand. The ring shift has maximum influence in deciding the position of redocked ligand. In such perspective ring shift was an appropriate consideration in the case of hydrophobic interaction.

Cocrystallized and redocked ligand conformation has its hydrophobic interaction in the same fashion and has limited ring shifts with slight torsion at the morpholinyl linkage. The hydrophobic interaction generated by the rings of LY294002 at the WPF shelf was directed at amino acids like Val87, Cys136, Leu92, Ile146, and Phe83. Table 3 shows the position (XYZ) of the ligand at the WPF shelf along with the type of hydrophobic bond. This explains the ring shift from the centre of gorge area with respect to the cocrystallized ligand.

3.2. Binding Affinity of Known Inhibitors and Investigational Ligands. Except JQ1, the binding affinity of known inhibitors was found to be less in comparison with flavonoids under study.

The resolution of crystal structures used and their cocrystallized ligand has been listed out in Table 2 along with docked energy (ΔG), amino acid residue interacted, and its distance in formation of hydrogen bond (Å).

Repeated docking analysis showed the reliability in docking and the known inhibitors occupying the WPF shelf with maximum conformity. Among them JQ1 exhibited a docked energy of −6.52 kcal/mol. In this conformation, there is a well oriented H-bond interaction with Asn140. The Ligplot (Figure 6) shows the occupancy of the known inhibitors at WPF shelf.

When analyzing investigational ligands, among them 3-O-acetylpinobanksin, naringenin triacetate, kaempferol tetraacetate, and artemetin acetate were found to show a binding affinity of −6.41, −6.29, −6.25, and −6.16 kcal/mol. Table 3 shows the docking score of investigational ligands.

Whereas, di-acetyl group substituted naringenin and 3-O-acetyl pinobanksin substituted with an extra acetyl group at C7 positionlag behind in scoring as −5.95 and −5.82 kcal/mol, respectively.

Native flavone moiety with differing hydroxy, methoxy, and acetyl substitution on C5, C7, and C8, namely, 5-hydroxy-7-acetoxy-8-methoxy flavone, exhibits a satisfactory binding

Table 3: Redocked ligand and cocrystallized ligand position at grid centre of crystal structure of BRD4 BD1. (The amino acid involved in hydrophobic interaction with LY294002 and its positioning with respect to the free energy of binding is shown according to its *XYZ*-axis.)

Serial number	Hydrophobic interaction	Cocrystallized ligand			Redocked ligand		
		X	*Y*	*Z*	*X*	*Y*	*Z*
1	A:PHE83 - :Ligand	−9.93	11.47	−9.27	−9.82	11.47	−9.03
2	Ligand - A:ILE146	−13.76	14.09	−3.43	−13.23	13.97	−3.21
3	Ligand - A:ILE146	−12.82	13.04	−5.51	−11.76	11.04	−5.45
4	Ligand - A:VAL87	−15.46	12.46	−9.05	−15.37	12.11	−9.05
5	Ligand - A:ILE146	−13.39	12.37	−4.67	−13.65	12.68	−4.29
6	Ligand - A:LEU92	−17.91	10.63	−5.93	−17.09	10.54	−5.64
7	Ligand - A:VAL87	−16.02	11.80	−8.21	−15.59	11.62	−7.21
8	A:CYS136 - :Ligand	−10.34	14.10	−8.92	−10.34	14.87	−7.95
9	A:VAL87 - :Ligand	−14.09	12.41	−10.65	−14.15	12.05	−10.87

Table 4: Docking score with the hydrogen bond interaction of rare flavonoids onto the detected binding site in crystal structure of 4CFK.

Serial number	Ligand	Docking score kcal/mol	Amino acids interacted through hydrogen bonding	H-bond length Å
01	3-O-Acetylpinobanksin	−6.41	MET132	1.87
			ASN135	2.30
			TYR97	1.84
			ASN140	1.94
02	Naringenin triacetate	−6.29	TYR97	3.45
03	Kaempferol tetraacetate	−6.25	TYR97	2.50
			CYS136	2.79
04	Artemetin acetate	−6.16	TYR97	3.28
05	Naringenin diacetate	−5.95	ASN140	1.88
			LYS91	2.35
06	3,7-O-Acetylpinobanksin	−5.82	ASN140	1.84
07	Jaceidin triacetate	−5.73	ASN140	2.02
08	5-Hydroxy-7-acetoxy-8-methoxy flavone	−5.68	ASN140	1.94
09	5,7-Diacetoxy flavone	−5.04	GLN85	2.11
			LYS91	2.30
10	5-Acetoxy-7-hyroxy flavone	−4.77	ASP88	2.30
			GLN85	2.14

Table 5: Docking score, amino acids interacted, and H-bond length of multiple crystal structure of BRD4 (BD1) with 3-O-acetylpinobanksin.

Serial number	Ligand	PDB	RMSD Å	Docking score kcal/mol	Amino acids interacted through hydrogen bonding	H-bond length Å
01	3-O-Acetylpinobanksin	3MXF	0.96	−6.38	MET105	2.21
					TYR97	1.89
					ASN140	2.10
02		3U5J	0.94	−6.29	MET132	2.29
					ASN140	1.84
03		4NUC	0.89	−6.44	TYR97	2.25
					ASN140	2.12
					MET132	1.97
04		4C66	1.00	−6.40	MET132	2.08
					TYR97	2.39
					ASN140	1.85

affinity but the values of 5, 7-diacetoxy flavone, 5-acetoxy-7-hyroxy flavone show a reduction in docking score. It is evident from Table 4 which shows their docking score along with the dissociation constant.

The top scored ligand (3-O-acetylpinobanksin) among 10 ligands was again subjected to redocking onto different crystal structures like 4C66, 4NUC, 3U5J, and 3MXF. Three of the crystal structures exhibited docking score (Table 5) ≥ 6.40 kcal/mol.

All bromodomains share a conserved left-handed helix bundle that is made out of four α helices, named **αZ**, **αA**, **αB**, and **αC**, respectively. The interhelical loop regions known

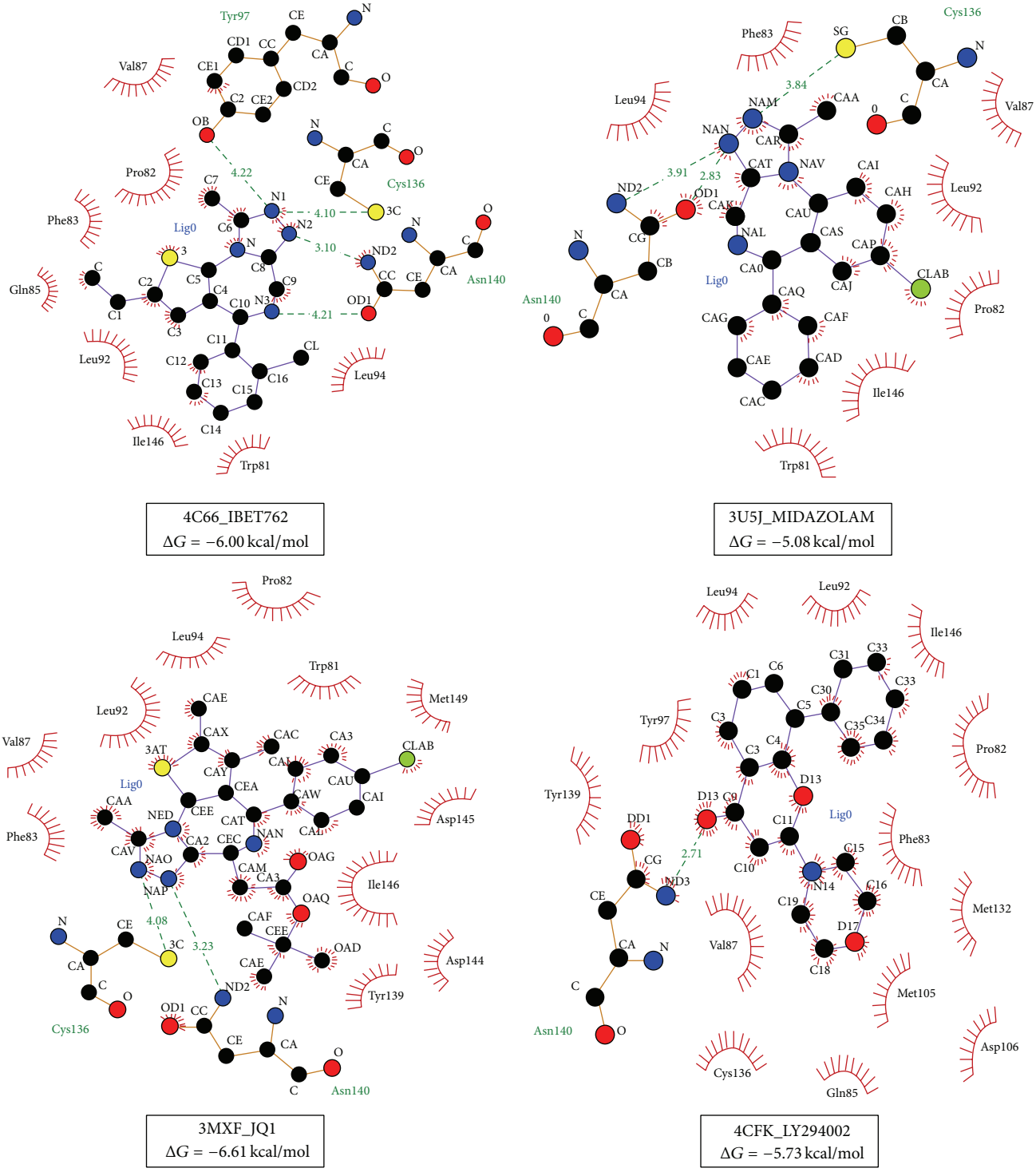

Figure 6: Ligplot image showing the occupancy and interaction of known inhibitors with its crystal structures. The image is generated using Ligplot plus version 1.4.5.

as the ZA and BC loops form the acetyl-lysine binding pocket located at one end of the helix bundle. The amino acid residues in the acetyl-lysine binding pocket are highly conserved with over 90% sequence identity between the two bromodomains in each BET protein. Of these is a highly conserved Asn residue that is essential for lysine-acetylated histone recognition by forming a hydrogen bond to the acetyl amide group of the acetylated lysine [15].

BRD4 BD1 binds to the acetylated H3 tail polypeptide at residues 12–19. Specifically, the conserved Asn140 in BD1

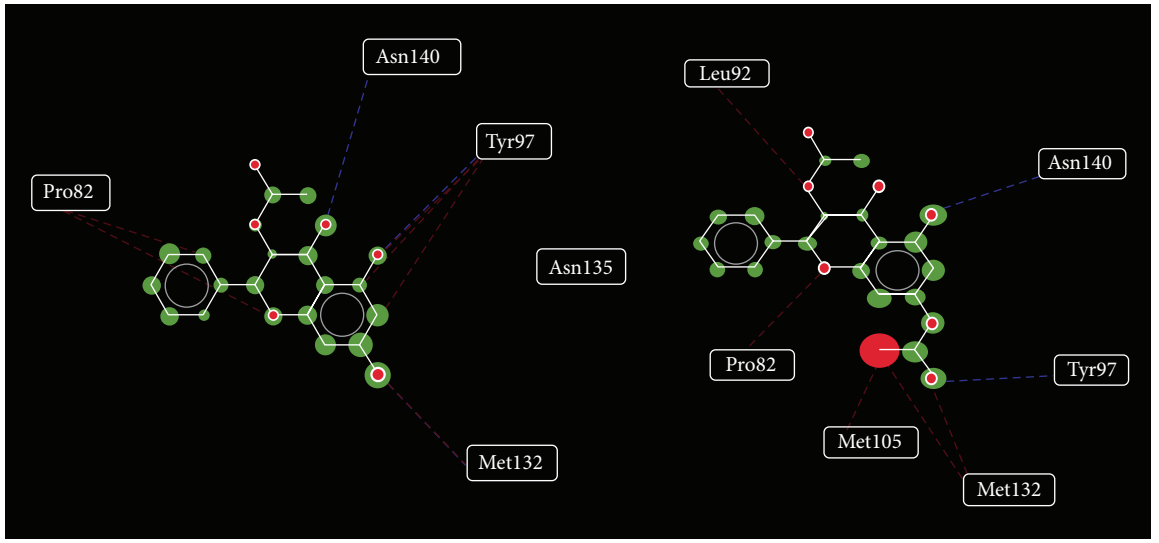

Figure 7: Ligand map showing hydrogen bond interaction (blue lines), steric interaction (red lines), and interaction overlay of 3-O-acetylpinobanksin (left) and 3,7-O-acetylpinobanksin (right). Image generated using Mole Gro molecular viewer 2.5 [27].

binds to the N_{zeta}-acetylated Lys14 in H3. Intermolecular hydrogen bonds are formed between the (O)η of the acetylated Lys14 and Asn140 of the BC loop. Water molecules surrounding the acetyl moiety orientate it so that there are hydrogen bonds between the hydroxy group of the Asn side chain and the backbone amide of the Ala residue in the histone peptide. Additional contacts with the acetylated lysine were mediated by Tyr139 and Ile46 and with Cys139 in some BRD4 BD1 [36].

The crystal structure with pdb code 4CFK was selected for docking analysis with rare flavonoids. In those selected pdb's, there was a conserved intermolecular hydrogen bonding between the amino acid residues in protein structure that was observed. Important hydrogen bond interactions within the amino acid residues of bromodomain at the Kac site were Asn140 and Cys136. Focusing on crystal structure of 4CFK, it showed an N-terminus commencing with Ser42 and continue as alpha-A helix at Asn61. Helical structure extends up to His77, where it has a slight coil and lengthens up to Asp106. In between this helix, residues form an AB loop (Gln78-Met105) and continue as alpha-B helix to descend at Asn116. The successive residues Asn117-Ala122 form a BC loop and then from Gln123 extend as alpha C helix up to Asn162.

Validation of docking methodology was performed in order to measure the reliability of molecular docking. Root-mean-squared deviation (RMSD) between the docked structure and the original conformation of the inhibitor in each complex was calculated. The RMSD of the docked pose is less than 1.0 Å from the experimentally observed conformation; this exhibits a successful prediction. From the binding poses and superimposition of docked conformation of the ligand, the prediction was said to be accurate.

Selected flavonoids contain methoxy, hydroxyl, and acetyl groups. Binding characteristics at the acetylation gorge of BRD4 BD1 were evaluated in comparison with known inhibitors

Selective rare flavonoids showed their interaction with the amino acids residues of predicted binding site of BC loop. Ligand map (Figures 7, 11, and 14) shows the hydrogen bond and steric interactions of the ligand with the bromodomain. It is a planar ligand map where only one set of interactions are visible and it has been shown in following discussion.

The binding free energy was mainly accounted for by hydrophobic interactions, while electrostatic forces might contribute to the specificity of the interaction. Thus affinity constant is independent of the ionic strength [37]. Hence hydrophobic interactions have been visualized and their importance is discussed throughout the binding interaction analysis.

Among those selective rare flavonoids and in comparison with known inhibitors, 3-O-acetylpinobanksin has a lowest binding energy (ΔG) of −6.41 kcal/mol. 3-O-Acetylpinobanksin is a (2R, 3R)-2-cyclohexyl-5,7-dimethyl-3-(prop-1-en-2-yloxy)-octahydro-2H-1-benzopyran-4-one. Figures 7 and 8 show the interaction of 3-O-acetylpinobanksin at the Kac site. Oxygen atom of C4 and C5 provoke an acceptance of H-bond at Asn140 (1.94 Å) and Tyr97 (1.84 Å) respectively, whereas hydroxyl group of C7and C5 act as hydrogen bond donors to interact with Met132 (1.87 Å) and Asn135 (2.30 Å). Steric interactions are a type of hydrophobic interactions prominent in a structural manner.

C2 substituted (2R, 3R)-2-cyclohexyl moiety has its unidirectional hydrophobic interactions from Pro82 and a bidirectional force of attraction with Leu92 and Val87. Figure 9 shows benzopyrone nucleus under the influence of Val87 holding a hydrophobic interaction with Ile146 and Cys136.

3,7-O-Acetylpinobanksin is a 3-(acetyloxy)-2-cyclohexyl-5-hydroxy-4-oxo-4a,5,6,7,8,8a-hexahydro-4H-chromen-7-yl acetate. There was a hydrogen bond acceptor interaction from Tyr97 with terminal methyl group of acetyl moiety at C7 position of 3,7-O-acetylpinobanksin. When comparing with 3-O-acetylpinobanksin, residue Asn140 (1.84 Å) switched

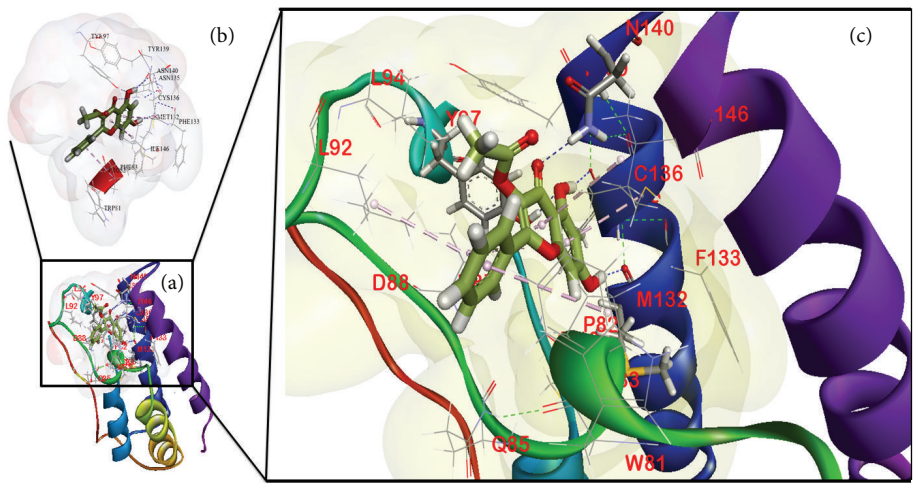

Figure 8: Emphasized image shows the binding interaction of 3-O-acetylpinobanksin at N-acetyl-lysine binding site of BD1 domain of BRD4 family protein. Image generated using Accelrys' discovery studio 4.0 [25]. (a) Secondary structure showing the ligand at the WPF shelf with surface around cavity. (b) The cavity area is shown as a transparent surface with ligand. (c) The emphasized image showing the H-bond interaction (dark blue lines) and hydrophobic interaction (sky blue cylindrical lines) of amino acid residues [shown as sticks (0.20 Å) and lines, resp.] with the ligands.

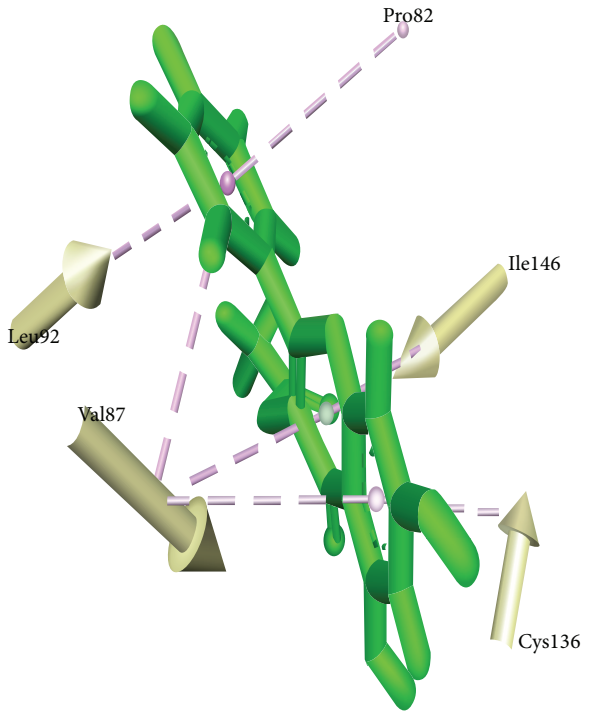

Figure 9: 3-O-Acetylpinobanksin. Hydrophobic interactions of C2 substituted (2R, 3R)-2-cyclo-hexyl moiety have their unidirectional hydrophobic interactions from Pro82 and a bidirectional force of attraction with Leu92 and Val87 is projected. Benzopyrone nucleus under the influence of Val87 holds a hydrophobic interaction with Ile146 and Cys136. Image is generated using Accelrys' discovery studio 4.0 [25].

away its interaction from pyran to adhering fused 5, 7 hydroxy benzene but there was a conserved hydrophobic interaction between Met132 and C7 acetyl group in both forms of Pinobanksin. Electrostatic interaction is highly visible from Met130 and a prominent H-bond from Tyr97 with C7 acetyl group.

There was a predicted binding mode of acetyl mimics in BRD4. It is characterized by a lipophilic sandwich of their bicyclic core between residues Val87, Leu92, Leu94, and Tyr97 on one side and Phe83 and Ile146 on the other side of the binding pocket [38]. The carbonyl oxygen of both compounds is engaged in hydrogen bonding interactions with the highly conserved Asn140, a typical feature among bromodomain inhibitors as most of them are acetyl-lysine mimics [39–45].

Naringenin triacetate is a 5-(acetyloxy)-2-[4-(acetyloxy) cyclohexyl]-4-oxo- 4a, 5,6,7,8,8a-hexa hydro-4H-chromen-7-yl acetate naringenin triacetate at its free energy of binding (−6.29 kcal/mol) that showed dominancy of hydrophobic interaction rather than hydrogen bond interaction. The hydrogen bond distance formed by oxygen atom of C4′ substituted acetyloxy moiety with Tyr97 (3.45 Å) was found to be very weak (−0.65 kcal/mol) but due to the existence of nonbond interactions between ligand and residues of BRD4 BD1, binding affinity was stronger. C2 branched 4-acetyloxy cyclohexyl moiety on its perpendicular axis has its steric interactions in three directions via Pro82 (5.05Å), Leu92 (4.94 Å), and Val87 (5.23 Å); on the other side Phe83 directly interacts with carbonyl oxygen from 4-acetyl of cyclohexyl moiety.

An investigation on compounds like acetyl mimics was predicted to further occupy the hydrophobic WPF shelf, which is an important region for ligand design to gain potency [38].

In turn Val 87 (4.20 Å) also has steric interaction with benzopyrone nucleus. The other side of the benzopyrone nucleus receives hydrophobic interaction from Cys136 (4.21 Å), Ile146 (4.81 Å), and Phe83. Figure 10 explains the difference in pose generated hydrophobic interaction of naringenin triacetate and 3-O-acetylpinobanksin on the reasoning of free energy of binding (ΔG).

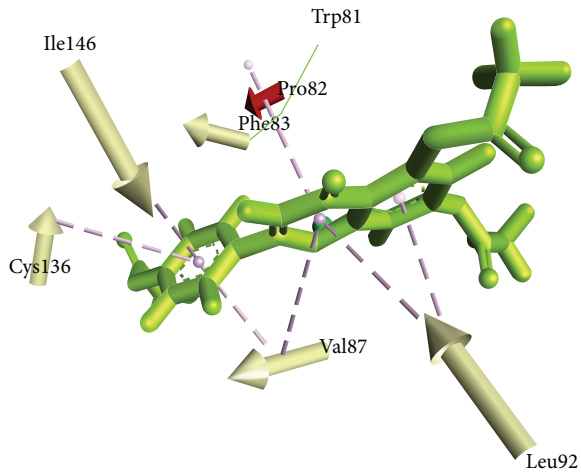

Figure 10: Naringenin triacetate. C2 branched 4-acetyloxy cyclohexyl moiety on its perpendicular axis has its steric interactions in three directions via Pro82, Leu92, and Val87. On the other side Phe83 directly interacts with carbonyl oxygen from 4-acetyl of cyclohexyl moiety. Image generated using Accelrys' discovery studio 4.0 [25].

Ligand map from Figure 11 projects the hydrogen bonding interaction of kaempferol tetraacetate, Jaceidin triacetate, and naringenin diacetate. Discussing naringenin triacetate and naringenin diacetate shows the impact of acetyl groups at various positions and naringenin diacetate is a 2-[4-(acetyloxy)cyclohexyl]-5-hydroxy-4-oxo-4a,5,6,7,8,8a-hexahydro-4H-chromen-7-yl acetate. C2 position with 4-acetyloxy cyclohexyl moiety and hydroxyl group at C7 of benzopyrone nucleus interacts effectively through hydrogen binding with Lys91 (2.35 Å) and Asn140 (1.88 Å). Even though there was a classical interaction of Asn140, there was considerably less binding affinity, but its binding energy is comparable with known inhibitors like midazolam, alprazolam, and GSK525762 [46]. The acetyl group at 4-(acetyloxy) cyclohexyl moiety substituted at C2 position of benzopyrone nucleus has maximum influence in generating binding potential in naringenin diacetate and triacetate through nonbonding interactions.

Kaempferol tetraacetate is a 3,5-bis(acetyloxy)-2-[4-(acetyloxy) cyclohexyl]-4-oxo-4a,5,6,7,8,8a-hexahydro-4H-chromen-7-yl acetate. Acetyl group of 4-(acetyloxy) cyclohexyl moiety interacts at Tyr97 (2.50 Å) through hydrogen bonding and as well as with a steric interaction. In case of jaceidin triacetate, at the same position there is a void of interaction with expected Tyr97; this might be due to the presence of methoxy group at the adjacent carbon (C5′). This screening effect would prohibit strain along the ring and make both the oxygen atoms at carbonyl oxygen (O–C=O) of acetyl group at C7 induce a force of nonbond hydrogen bond interaction at Asn140 (2.02 Å)and Steric interaction with Val87. Hydrophobic moments along the interaction field were found to have the same symmetry like 3-O-acetylpinobanksin but due to the position of acetyl groups their nonbond interaction varies considerably and elicits free energy of binding. This explains the strain created along the bonds due to methoxy groups and acetyl groups in the ligands at the gorge environment.

RVX-208 binds BRD4 BD1 in a mostly hydrophobic pocket where it is flanked by Val87, Leu92, and Leu94 side chains on one side of the compound and Pro82 and Leu146 side chain on the other. It is also within van der Waals distances to the four aromatic residues Tyr97, Tyr139, Phe83, and Trp81. RVX-208 is a quinazolin-4-one it forms a bidentate set of two hydrogen bond interactions with the conserved Asn140 amide side chain and the amino acid recognized by acetylated lysine of the natural substrate, as well as an extensive water network. The quinazolin-4-one scaffold ketone and methoxy oxygens both form a water-mediated interaction with the Tyr97 hydroxyl group [47].

Comparison of this type of interaction with artemetin acetate raises a quite discriminative interaction. Artemetin acetate is a 2-(3,4-dimethoxycyclohexyl)-3,6,7,8-tetramethoxy-4-oxo-4a,5,6,7,8,8a-hexahydro-4H-chromen-5-yl acetate. Artemetin acetate contain almost 5 methoxy groups in the entire structure, among them only oxygen atom of methoxy group at C5′ was involved in nonbonding interaction, but adjacent acetyl group at C4′ showed a significant interaction at Tyr97 (3.28 Å) and type of interaction was absent in jaceidin triacetate. Simultaneously artemetin acetate has strong hydrophobic interactions (Figure 12) due to the presence of acetyl groups, which exhibit overall binding affinity of 6.16 kcal/mol compared to jaceidin triacetate, which is involved in Asn140 interaction.

Diazobenzene inhibitors bind across the acetyl-lysine binding pocket in the ZA and BC loops in the BRD4 BD1. The hydroxyl group in the A ring forms a hydrogen bond to the amide of the conserved Asn140 and another water (W1) mediated hydrogen bond to the phenoxyl group for Tyr97 [15].

Some set of structurally optimized flavonoids bearing a common flavone nucleus with acetyl, methoxy, and hydroxyl groups specifically at C5, C7, and C8 positions like 5-hydroxy-7-acetoxy-8-methoxy flavone, 5-acetoxy-7-hyroxy flavone, and 5,7-diacetoxy flavone were evaluated through docking for their affinity in accessing the lysine binding site of bromodomains.

5-Hydroxy-7-acetoxy-8-methoxy flavone is a 2-cyclohexyl-5-hydroxy-8-methoxy-4-oxo-4a,5,6,7,8,8a-hexahydro-4H-chromen-7-yl acetate and has showed a considerable free energy of binding (5.68 kcal/mol) with efficient hydrogen bonding with Asn140 (1.94 Å). Distance produced by 3-O-acetylpinobanksin and 5-hydroxy-7-acetoxy-8-methoxy flavone through C4 and C5 hydroxyl groups in forming H-bond was found to be the same. The binding energy of former is less, due to the lack of additional hydrogen bonding. The steric interactions with Pro82, Phe83, Tyr97, Met132, Met105, and Asn135 enhanced the affinity of binding. Their hydrophobic moment is shown in Figure 13. Tyr 97 was found to show hydrophobic interaction abundance with the ligand. This can be explained more clearly than the ligand map as shown in Figure 14.

5-Acetoxy-7-hyroxy flavone and 5,7-diacetoxy flavone containing hydroxyl groups showed a similar type of interaction with Gln85 (2.11 Å and 2.14 Å) and a hydrophobic

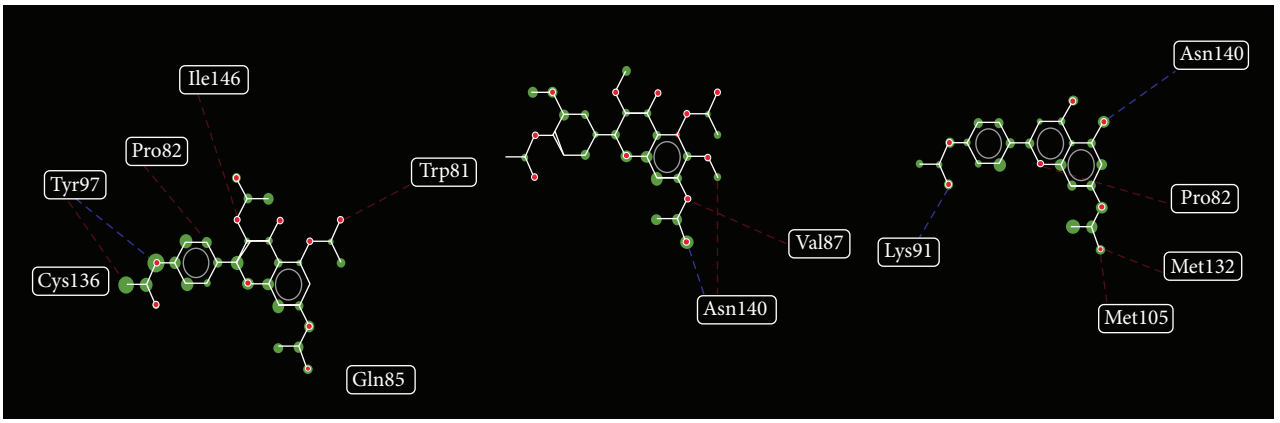

Figure 11: Ligand map showing the hydrogen bonding (blue lines), steric interactions (red lines), and interaction overlay of kaempferol tetraacetate (left), jacedin triacetate (middle), and naringenin diacetate (right). Image generated using Mole Gro molecular viewer 2.5.

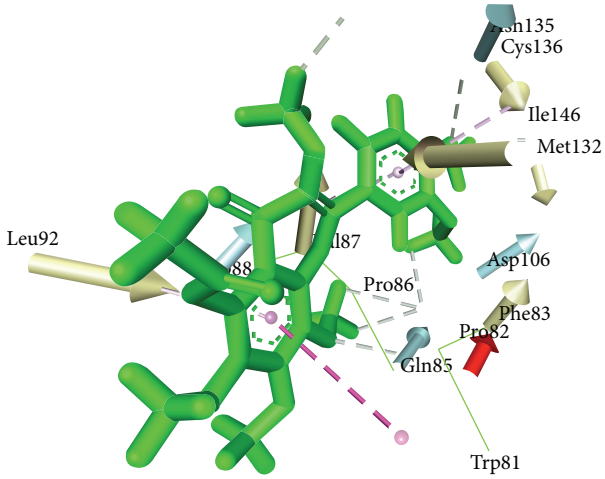

Figure 12: The hydrophobic moments showing the multiple nonbond interaction with artemetin acetate at the gorge area interactions.

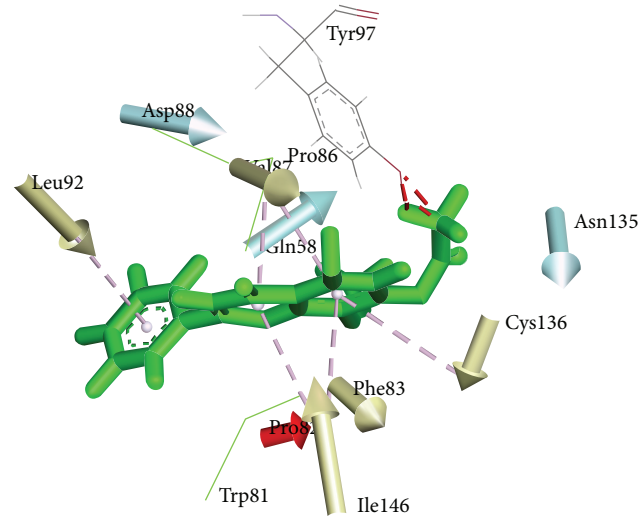

Figure 13: 5-Hydroxy-7-acetoxy-8-methoxy flavone. The steric interactions with Pro82, Phe83, Tyr97, Met132, Met105, and Asn135 enhanced the affinity of binding. Tyr 97 was found to show hydrophobic interaction abundance with 5-hydroxyl-7-acetoxy-8-methoxy flavone.

interaction with Pro82; this shows the reliability in binding affinity of the scoring function. Hydroxyl and acetyl groups in both of these compounds have variation in H-bond formation. In 5,7-diacetoxy flavone, an acetyl group at C7 dominates in Lys91 (2.30 Å) interaction but when C7 position is replaced with a hydroxyl group to contour a 5-acetoxy-7-hydroxy flavone, there is a lack of interaction with Lys91 and acetyl group at C5 induced a nonbond interaction with Asp88 (2.30 Å). Focusing on these replacements, 5,7-diacetoxy flavone is occupied with maximum affinity in binding with classical Lys91 residue.

The drug can be made highly selective because of the ZA loops and the WPF shelf outside of the acetyl-lysine binding pocket. Furthermore, the conserved Ile or Val imposes spatial constraints on the size of molecules that can gain access to the WPF shelf. The binding of BD1 shows stereoselectivity because the enantiomer form of I-BET (GSK525768A) cannot bind to BD1 and shows no activity towards BET. By binding to the Lys binding pocket, I-BET can block the binding of the acetylated Lys14 in histone to BRD4 BD1, thereby preventing gene expression [48].

Being a best scored ligand, 3-O-acetylpinobanksin was examined for redocking on multiple crystal structures with different resolution, namely, 3U5J, 3MXF, 4CFK, and 4C66 to know the reliability in their access towards ε-N-acetyl-lysine binding site. Table 5 shows their binding energy with its interacting amino acids and Figure 15 shows the ligand map of 3-O-acetylpinobanksin with different crystal structures.

The critical amino acid residue of importance is Asn140 AND Tyr97. On analysing the interaction of investigational ligands with 4CFK and specific interaction of 3-O-acetylpinobanksin with different crystal structures, there was a slight difference in the locations of the interacting (H-bonding) amino acid residues with the ligands. This

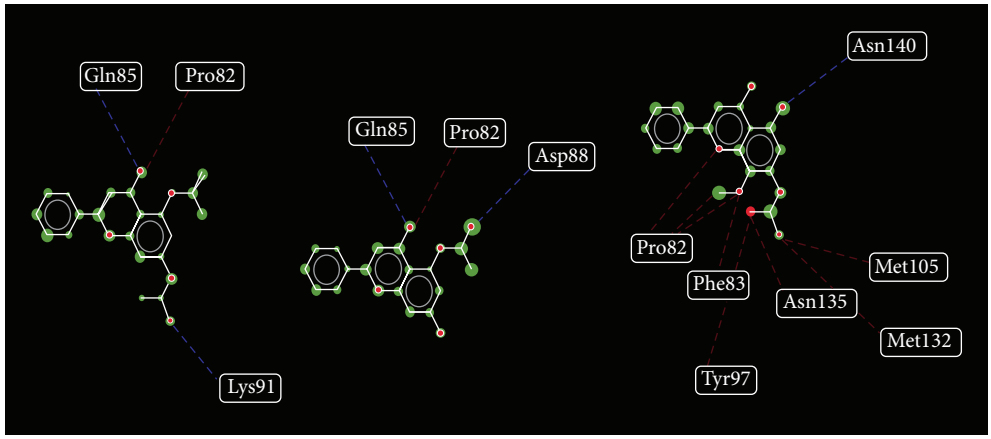

Figure 14: Ligand map showing the hydrogen bonding (blue lines), steric interactions (red lines), and interaction overlay of interaction of 5, 7-diacetoxy flavone (left), 5-acetoxy-7-hydroxy flavone (middle), and 5-hydroxy-7-acetoxy-8-methoxy flavone (right). Image generated using Mole Gro molecular viewer 2.5.

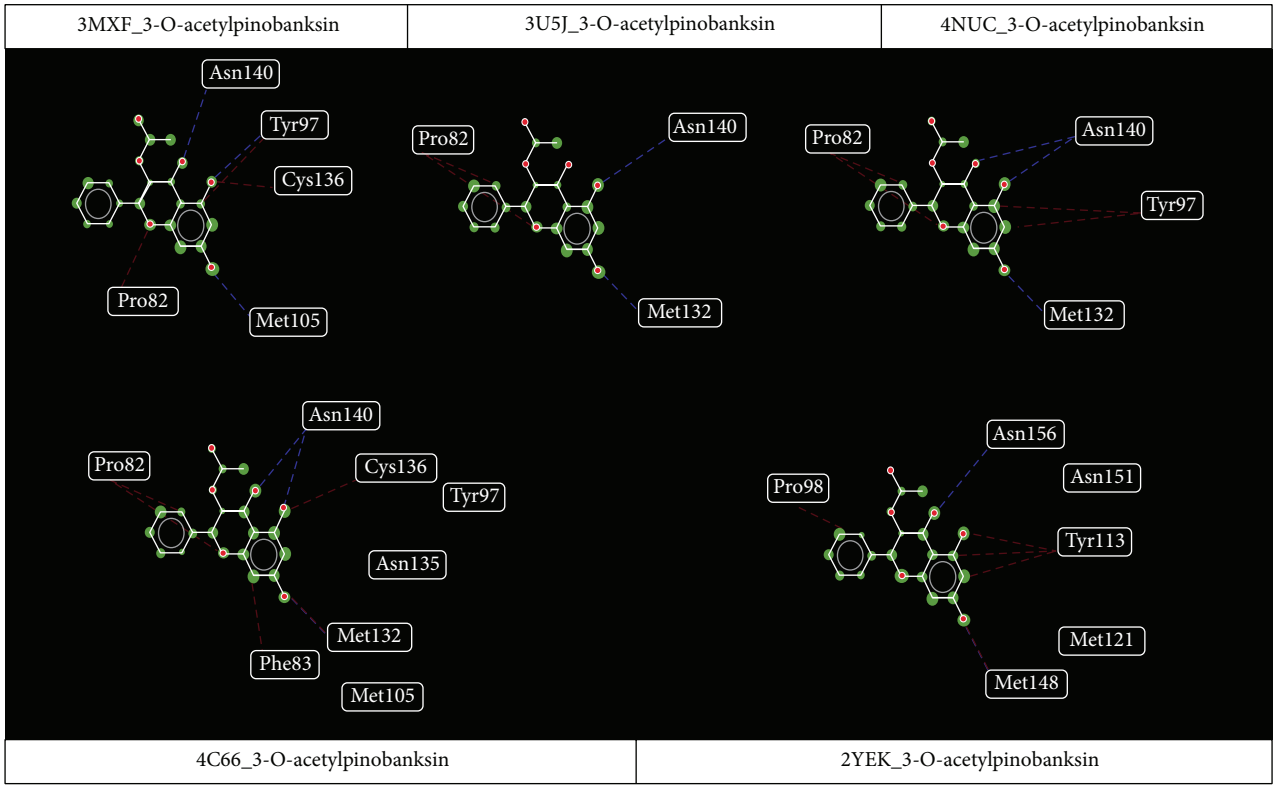

Figure 15: Ligand map of 3-O-acetylpinobanksin with multiple crystal structures of BD1 domains of BRD4. Image generated using Mole Gro molecular viewer 2.5.

was evidenced by the distance of hydrogen bonds formed between the ligand and the residues. 3-O-Acetylpinobanksin and 5-hydroxyl-7-acetoxy-8-methoxy flavone shared a common distance of 1.94 Å whereas naringenin diacetate, 3,7-O-acetylpinobanksin made interaction at a distance of 1.84 Å. There was a 0.10 Å difference in every set of interactions among the investigational ligands. On comparison, the specific interaction of 3-O-acetylpinobanksin with different crystal structures as shown in Table 5 also exhibited a 0.10 Å distance variation.

Overlapping analysis of investigational ligands with a reported known inhibitor, LY294002, with a benzopyran nucleus is done in order to know about the structural efficiency of rare flavonoids in occupying the binding site area. Then analysis is made on the necessary structural importance of rare flavonoids in bromodomain binding. Figure 16 shows the evidence for superimposition of 3-O-acetylpinobanksin and LY294002.

Flavonoids occupy the WPF shelf and nonbonding interaction was also found at these areas with the investigational

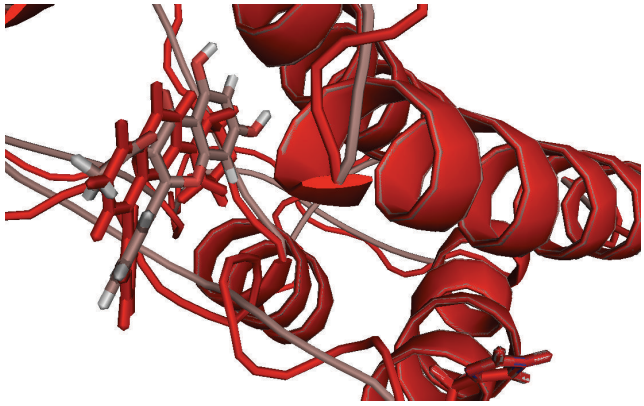

Figure 16: Image displayed is showing the crystal structure of 4CFK containing its cocrystallized ligand (LY294002) overlapped onto the energy minimized 4CFK with docked 3-O-acetylpinobanksin. Red colour is LY294002 and red salmon 3-O-acetylpinobanksin; those colors mentioned are the same for protein structure and cocrystallized ligand [image is generated using PyMOL viewer].

ligands without disturbing the intramolecular hydrogen bonding in the domain structures.

It is concluded that selective rare flavonoids like 3-O-acetylpinobanksin, naringenin diacetate, and kaempferol tetraacetate were found to occupy the WPF shelf with maximum fidelity and with satisfactory binding energy (ΔG). Substitution of acetyl, methoxy, and hydroxyl group on benzopyrone structures shows influence in binding interaction at Kac site. Most of the investigational ligands interacted at Asn140, Tyr97, Met132, and Lys91 through nonbonding interactions like steric interactions and hydrophobic interaction. In that perspective, these compounds would act as a better BRD4 BD1 inhibitor. Further *in vitro* and *in vivo* studies can be carried out in order to produce supporting information and can target the inhabitation of bromodomains, the epigenetic readers of lysine acetylation.

Conflict of Interests

The author has no conflict of interests.

Acknowledgment

The author acknowledges Dr. Hong Tao Zhao Ph.D, Scientist, Medivir AB, Stockholm County, Sweden, for giving valuable suggestion on the usage of docking software, LeDock.

References

[1] G. Drewes, "Future strategies in epigenetic drug discovery," *Drug Discovery Today: Therapeutic Strategies*, vol. 9, no. 2-3, pp. e121–e127, 2012.

[2] S. Picaud, C. Wells, I. Felletar et al., "RVX-208, an inhibitor of BET transcriptional regulators with selectivity for the second bromodomain," *Proceedings of the National Academy of Sciences of the United States of America*, vol. 110, no. 49, pp. 19754–19759, 2013.

[3] A. Dey, J. Ellenberg, A. Farina et al., "A bromodomain protein, MCAP, associates with mitotic chromosomes and affects G_2-to-M transition," *Molecular and Cellular Biology*, vol. 20, no. 17, pp. 6537–6549, 2000.

[4] T. Kanno, Y. Kanno, R. M. Siegel, M. K. Jang, M. J. Lenardo, and K. Ozato, "Selective recognition of acetylated histones by bromodomain proteins visualized in living cells," *Molecular Cell*, vol. 13, no. 1, pp. 33–43, 2004.

[5] A. Dey, F. Chitsaz, A. Abbasi, T. Misteli, and K. Ozato, "The double bromodomain protein Brd4 binds to acetylated chromatin during interphase and mitosis," *Proceedings of the National Academy of Sciences of the United States of America*, vol. 100, no. 15, pp. 8758–8763, 2003.

[6] S. Muller, P. Filippakopoulos, and S. Knapp, "Bromodomains as therapeutic targets," *Expert Reviews in Molecular Medicine*, vol. 13, article e29, 2011.

[7] B. Florence and D. V. Faller, "You bet-cha: a novel family of transcriptional regulators," *Frontiers in Bioscience*, vol. 6, pp. D1008–D1018, 2001.

[8] S.-Y. Wu and C.-M. Chiang, "The double bromodomain-containing chromatin adaptor Brd4 and transcriptional regulation," *Journal of Biological Chemistry*, vol. 282, no. 18, pp. 13141–13145, 2007.

[9] C. Choudhary, C. Kumar, F. Gnad et al., "Lysine acetylation targets protein complexes and co-regulates major cellular functions," *Science*, vol. 325, no. 5942, pp. 834–840, 2009.

[10] P. Filippakopoulos, J. Qi, S. Picaud et al., "Selective inhibition of BET bromodomains," *Nature*, vol. 468, no. 7327, pp. 1067–1073, 2010.

[11] C. W. Chung, H. Coste, J. H. White et al., "Discovery and characterization of small molecule inhibitors of the BET family bromodomains," *Journal of Medicinal Chemistry*, vol. 54, no. 11, pp. 3827–3838, 2011.

[12] P. Filippakopoulos, S. Picaud, M. Mangos et al., "Histone recognition and large-scale structural analysis of the human bromodomain family," *Cell*, vol. 149, no. 1, pp. 214–231, 2012.

[13] O. Mirguet, R. Gosmini, J. Toum et al., "Discovery of epigenetic regulator i-bet762: lead optimization to afford a clinical candidate inhibitor of the bet bromodomains," *Journal of Medicinal Chemistry*, vol. 56, no. 19, pp. 7501–7515, 2013.

[14] Y. Zhao, C.-Y. Yang, and S. Wang, "The making of i-bet762, a BET bromodomain inhibitor now in clinical development," *Journal of Medicinal Chemistry*, vol. 56, no. 19, pp. 7498–7500, 2013.

[15] G. Zhang, A. N. Plotnikov, E. Rusinova et al., "Structure-guided design of potent diazobenzene inhibitors for the BET bromodomains," *Journal of Medicinal Chemistry*, vol. 56, no. 22, pp. 9251–9264, 2013.

[16] A. Dittmann, T. Werner, C.-W. Chung et al., "The commonly used PI3-kinase probe LY294002 is an inhibitor of BET bromodomains," *ACS Chemical Biology*, vol. 9, no. 2, pp. 495–502, 2014.

[17] C. A. Lipinski, F. Lombardo, B. W. Dominy, and P. J. Feeney, "Experimental and computational approaches to estimate solubility and permeability in drug discovery and development settings," *Advanced Drug Delivery Reviews*, vol. 46, no. 1–3, pp. 3–26, 2001.

[18] H. M. Berman, J. Westbrook, Z. Feng et al., "The protein data bank," *Nucleic Acids Research*, vol. 28, no. 1, pp. 235–242, 2000.

[19] *ACD/Structure Elucidator, version 12.01*, Advanced Chemistry Development, Inc., Toronto, Canada, 2014, http://www.acdlabs.com.

[20] K. Dhananjayan, A. Sumathy, and S. Palanisamy, "Molecular docking studies and in-vitro acetylcholinesterase inhibition by terpenoids and flavonoids," *Asian Journal of Research in Chemistry*, vol. 6, no. 11, pp. 1011–1017, 2013.

[21] J. J. P. Stewart, "Optimization of parameters for semiempirical methods VI: more modifications to the NDDO approximations and re-optimization of parameters," *Journal of Molecular Modeling*, vol. 19, no. 1, pp. 1–32, 2013.

[22] N. Mills, "ChemDraw ultra 10.0 cambridgesoft, 100 cambridgepark drive, Cambridge, MA 02140. http://www.cambridgesoft.com/. Commercial price: $1910 for download, #150 for CD-ROM; academic price: $710 for download, $800 for CD-ROM," *Journal of the American Chemical Society*, vol. 128, no. 41, pp. 13649–13650, 2006.

[23] H. Zhao and A. Caflisch, "Discovery of ZAP70 inhibitors by high-throughput docking into a conformation of its kinase domain generated by molecular dynamics," *Bioorganic & Medicinal Chemistry Letters*, vol. 23, no. 20, pp. 5721–5726, 2013.

[24] D. Seeliger and B. L. De Groot, "Ligand docking and binding site analysis with PyMOL and Autodock/Vina," *Journal of Computer-Aided Molecular Design*, vol. 24, no. 5, pp. 417–422, 2010.

[25] Accelrys Software, *Discovery Studio Modeling Environment*, Release 4.0, Accelrys Software, San Diego, Calif, USA, 2013, http://accelrys.com/products/discovery-studio.

[26] R. Thomsen and M. H. Christensen, "MolDock: a new technique for high-accuracy molecular docking," *Journal of Medicinal Chemistry*, vol. 49, no. 11, pp. 3315–3321, 2006.

[27] D. Karthik, "Computational designing and molecular docking studyof bio-flavonoids against crystal structure of β-secretase (BACE-1) utilizing MolDock scoring function, a modified Piecewise linear Potential (PLP) scoring method," *Journal of Computational Methods in Molecular Design*, vol. 4, no. 2, pp. 57–68, 2014.

[28] A. C. Wallace, R. A. Laskowski, and J. M. Thornton, "LIGPLOT: a program to generate schematic diagrams of protein-ligand interactions," *Protein Engineering*, vol. 8, no. 2, pp. 127–134, 1995.

[29] F. F. Charlotte, "General Hartree-Fock program," *Computer Physics Communications*, vol. 43, no. 3, pp. 355–365, 1987.

[30] C. C. J. Roothaan, "New developments in molecular orbital theory," *Reviews of Modern Physics*, vol. 23, no. 2, pp. 69–89, 1951.

[31] R. S. Mulliken, "Electronic population analysis on LCAOMO molecular wave functions I," *The Journal of Chemical Physics*, vol. 23, no. 10, pp. 1833–1840, 1955.

[32] H. Zhao and D. Huang, "Hydrogen bonding penalty upon ligand binding," *PLoS ONE*, vol. 6, no. 6, Article ID e19923, 2011.

[33] N. M. O'Boyle, M. Banck, C. A. James, C. Morley, T. Vandermeersch, and G. R. Hutchison, "Open Babel: an open chemical toolbox," *Journal of Cheminformatics*, vol. 3, article 33, 2011.

[34] K. Dhananjayan, S. Arunachalam, P. Sivanandy, and M. Parameswaran, "Computational drug discovery of Rho—associated coiled coil kinase II (ROCK-II) inhibitors as a target for neurodegenerative disorders—an insilico docking studies," *Oriental Pharmacy and Experimental Medicine*, 2014.

[35] J. Wang, R. M. Wolf, J. W. Caldwell, P. A. Kollman, and D. A. Case, "Development and testing of a general AMBER force field," *Journal of Computational Chemistry*, vol. 25, no. 9, pp. 1157–1174, 2004.

[36] F. Vollmuth, W. Blankenfeldt, and M. Geyer, "Structures of the dual bromodomains of the P-TEFb-activating protein Brd4 at atomic resolution," *The Journal of Biological Chemistry*, vol. 284, no. 52, pp. 36547–36556, 2009.

[37] P. Bongrand, "Ligand–receptor interactions," *Reports on Progress in Physics*, vol. 62, no. 6, article 921, 1999.

[38] H. Zhao, L. Gartenmann, J. Dong, D. Spiliotopoulos, and A. Caflisch, "Discovery of BRD4 bromodomain inhibitors by fragment-based high-throughput docking," *Bioorganic and Medicinal Chemistry Letters*, vol. 24, no. 11, pp. 2493–2496, 2014.

[39] C.-W. Chung, A. W. Dean, J. M. Woolven, and P. J. Bamborough, "Fragment-based discovery of bromodomain inhibitors part 1: inhibitor binding modes and implications for lead discovery," *Journal of Medicinal Chemistry*, vol. 55, no. 2, pp. 576–586, 2012.

[40] P. Bamborough, H. Diallo, J. D. Goodacre et al., "Fragment-based discovery of bromodomain inhibitors part 2: optimization of phenylisoxazole sulfonamides," *Journal of Medicinal Chemistry*, vol. 55, no. 2, pp. 587–596, 2012.

[41] L. Zhao, D. Cao, T. Chen et al., "Fragment-based drug discovery of 2-thiazolidinones as inhibitors of the histone reader BRD4 bromodomain," *Journal of Medicinal Chemistry*, vol. 56, no. 10, pp. 3833–3851, 2013.

[42] P. V. Fish, P. Filippakopoulos, G. Bish et al., "Identification of a chemical probe for bromo and extra C-terminal bromodomain inhibition through optimization of a fragment-derived hit," *Journal of Medicinal Chemistry*, vol. 55, no. 22, pp. 9831–9837, 2012.

[43] J.-M. Garnier, P. P. Sharp, and C. J. Burns, "BET bromodomain inhibitors: a patent review," *Expert Opinion on Therapeutic Patents*, vol. 24, no. 2, pp. 185–199, 2014.

[44] X. Lucas, D. Wohlwend, M. Hügle et al., "4-Acyl pyrroles: mimicking acetylated lysines in histone code reading," *Angewandte Chemie International Edition*, vol. 52, no. 52, pp. 14055–14059, 2013.

[45] B. A. Posner, H. Xi, and J. E. J. Mills, "Enhanced HTS hit selection via a local hit rate analysis," *Journal of Chemical Information and Modeling*, vol. 49, no. 10, pp. 2202–2210, 2009.

[46] L. R. Vidler, P. Filippakopoulos, O. Fedorov et al., "Discovery of novel small-molecule inhibitors of BRD4 using structure-based virtual screening," *Journal of Medicinal Chemistry*, vol. 56, no. 20, pp. 8073–8088, 2013.

[47] K. G. McLure, E. M. Gesner, L. Tsujikawa et al., "RVX-208, an inducer of ApoA-I in humans, is a BET bromodomain antagonist," *PLoS ONE*, vol. 8, no. 12, Article ID e83190, 2013.

[48] E. Nicodeme, K. L. Jeffrey, U. Schaefer et al., "Suppression of inflammation by a synthetic histone mimic," *Nature*, vol. 468, no. 7327, pp. 1119–1123, 2010.

[49] S. R. Haynes, C. Dollard, F. Winston, S. Beck, J. Trowsdale, and I. B. Dawid, "The bromodomain: a conserved sequence found in human, *Drosophila* and yeast proteins," *Nucleic Acids Research*, vol. 20, no. 10, article 2603, 1992.